Original Article

Triptolide Induces Apoptosis and Synergizes with Cisplatin in Cisplatin-Resistant HNE1/DDP Nasopharyngeal Cancer Cells

(triptolide / nasopharyngeal cancer / cisplatin resistance / reactive oxygen species, apoptosis)

X. WANG[1], J.-J. ZHANG[2], Y.-M. SUN[1], J. ZHANG[1], L.-R. WANG[3], J.-C. LI[1], H. LIU[1]

[1]Faculty of Pharmacy, Bengbu Medical College, [2]Department of Medical Oncology, the First Affiliated Hospital of Bengbu Medical College, Bengbu Anhui, China
[3]Department of Pharmaceutical Sciences, School of Pharmacy, Computational Chemical Genomics Screening Center, Pittsburgh, Pennsylvania, USA

Abstract. The purpose of the study was to evaluate the anti-tumour effects of triptolide (TPL) and of the combination of TPL and cisplatin (DDP) in DDP-resistant HNE1/DDP nasopharyngeal cancer (NPC) cells and to reveal the possible mechanisms. HNE1/DDP cells were treated with TPL and/or DDP. Cell proliferation was examined by 3-(4,5-dimethylthiazol-2-yl)-2,5-diphenyltetrazolium bromide (MTT) assay and colony-forming assay; the combination index of the synergism between TPL and DDP was calculated. Cell morphological changes were observed under a microscope. Reactive oxygen species (ROS) and apoptosis rate were determined by flow cytometry. 5,5',6,6'-tetrachloro-1,1',3,3'-tetrethyl benzimidalyl carbocyanine iodide (JC-1) staining was used to determine mitochondrial membrane potential (MMP). Protein expression was analysed by Western blot, including Bax, caspase-9, Bcl-2, Mcl-1. TPL had an obvious anti-tumour effect and exhibited synergistic cytotoxicity with DDP on DDP-resistant HNE1/ DDP cells. TPL induced HNE1/DDP cell apoptosis via inducing ROS generation. This effect was abolished by the inhibitor of ROS, N-acetyl-L-cysteine (NAC). TPL alone or combined with DDP could lower MMP significantly. Western blot showed that TPL alone or in combination with DDP increased expression of Bax and caspase-9, but reduced expression of Bcl-2 and Mcl-1. We conclude that TPL could induce cell apoptosis and synergize with DDP by regulating ROS generation and mitochondrial pathways in HNE1/DDP cells. This indicates that TPL may be effective in DDP-resistant NPC, either alone or combined with DDP.

Introduction

Nasopharyngeal cancer (NPC) is a malignant tumour occurring in the top and side walls of the nasopharyngeal cavity. Every year, 80,000 new cases of NPC are diagnosed worldwide and 50,000 individuals die of this disease. Over 80 % of these cases are from Asian countries, especially China and other Southeast Asia countries (Marquitz et al., 2012; Sun et al., 2014). Radiotherapy and adjuvant DDP chemotherapy are the main treatment options for NPC (Pan et al., 2013). However, DDP resistance usually develops during NPC therapy and results in the failure of radiotherapy and adjuvant DDP chemotherapy for NPC (Feng et al., 2014; Su et al., 2014). There is a critical need to develop more effective treatments for NPC.

TPL, a diterpenoid triepoxide, is isolated from the root of Tripterygium Wilfordii Hook F (TWHF), which is a Chinese traditional medicine. Since it was successfully isolated and structurally characterized (Fig. 1) in 1972, TPL has attracted attention from researchers worldwide (Liu, 2011). Their findings revealed that TPL has various pharmacological effects, such as anti-inflammatory, anti-rheumatic, anti-tumour, anti-microbial, cardiovascular protective and anti-senile dementia properties (Li et al., 2014). This indicated that TPL can not only inhibit tumour growth directly *in vitro* and *in*

Fig. 1. Structure of TPL

vivo, but also enhance the anti-tumour effects of cyto-toxic agents and chemotherapeutic agents (Li et al., 2012; Alsaied et al., 2014). However, the effect of TPL on drug resistance of NPC has not been reported. The present study aimed to investigate whether TPL can inhibit cell proliferation and sensitize DDP in a DDP-resistant NPC cell line, and to explore the molecular signalling pathway triggered by TPL in DDP-resistant NPC cells. We further hypothesized that TPL can increase ROS accumulation, activate mitochondrial pathways, and promote apoptosis of the NPC cells. In this study, the HNE1/DDP cell line, which is an acquired drug-resistance NPC cell line, was used to investigate the inhibitory effect of TPL and its synergistic effect with DDP in drug-resistant NPC.

Material and Methods

Material

TPL (Tianjin Medical Co.,Ltd, TianJin, CHINA) was dissolved as a stock solution in dimethyl sulphoxide (DMSO) and freshly diluted in 5 mmol·l⁻¹ culture medium prior to use. DDP (QiLu Pharmacy Co., Ltd, Jinan, China), n-acetyl-L-cysteine (NAC), MTT, and propidium iodide (PI) were obtained from Sigma (Sigma-Aldrich, St Louis, MO). ROS fluorescent probe – dihydroethidium (DHE) was purchased from Vigorous Biotechnology (Beijing, China). JC-1, Rabbit monoclonal anti-Bcl-2 (1 : 1000), rabbit monoclonal anti-Mcl-1 (1 : 4000) and mouse monoclonal anti-β-actin (1 : 1000) antibodies were purchased from Santa Cruz Biotechnology (Santa Cruz, CA), and rabbit polyclonal anti-caspase 9 (1 : 500) and rabbit monoclonal anti-bax (1 : 500) antibodies were purchased from Cell Signaling Technology (Santa Cruz).

Cell culture

The human NPC-derived DDP resistant HNE1/DDP cell line was offered by the biochemical pharmacology experiment centre of Bengbu Medical College (Bengbu, China). To maintain the acquired resistance to DDP, the cells were cultured in RPMI-1640 medium supplemented with foetal bovine serum (10%), penicillin/streptomycin (100 U/ml) and DDP (3.2 μM) in a 5% humidified CO₂ atmosphere at 37 °C.

Cell viability assay

Cell viability was evaluated by MTT assay (Zhou et al., 2011). Briefly, 5 × 10³ cells per well were seeded in 96-well plates. Following drug treatment, cells were incubated with 15 μl MTT (5 mg/ml) for an additional 4 h. Then the medium was discarded and 150 μl DMSO was added to each well; cells were incubated in 37 °C for 30 min. Finally, the optical density of each well was measured at 570 nm using a Microplate Reader (BioTek, Winooski, VI). The interaction between TPL and DDP was quantified by the combination index (CI), which was calculated by the equation: CI = (D)1/(Dx)1 +(D)2/(Dx)2, where (Dx)1 and (Dx)2 indicate the individual dose of TPL and DDP required to inhibit a given level of cell growth, and (D)1 and (D)2 are the doses of TPL and DDP necessary to produce the same effect in combination, respectively (Li et al ., 2012).

Morphological changes

Exponentially growing HNE1/DDP cells were seeded in 12-well plates, 100,000 cells per well. After adhesion overnight, cells were treated with 0–80 nmol·l⁻¹ TPL for 24 h. Then, the cellular morphology was observed with an AxioCam HRC CCD camera (Olympus, Tokyo, Japan).

In vitro colony-forming assay

Fresh suspensions of HNE1/DDP cells were seeded at 5000 cells per well in a 6-well plate. The first medium change was done after the first five days. Subsequently, medium was changed every 3–4 days. Colonies were monitored microscopically to ensure that they were derived from single cells. Cultures were terminated at 14 days and stained with 1% crystal violet.

ROS detection

The changes in the intracellular ROS levels were determined by the ROS fluorescent probe DHE. Non-fluorescent DHE is cell-permeable and oxidized in the presence of ROS to form ethidium oxide. The ethidium oxides can incorporate into DNA and produce red fluorescence. Cells were seeded in a 6-well plate, 2 × 10⁵ cells per well, and attached overnight (Deeb et al., 2010). After treatments, cells were incubated with 5 μmol·l⁻¹ ROS fluorescent probe DHE for 2 h at 37 °C prior to being harvested and analysed by flow cytometry.

Cell apoptosis induced by TPL evaluated by PI staining

Cells were seeded in a 6-well plate at a density of 3 × 10⁵ cells per well (Bao et al., 2012). After overnight attachment, cells were treated with NAC and different concentrations of TPL. At the end of the treatment cells were digested by trypsin, washed with cold PBS, and fixed overnight with alcohol solution at 4 °C. Then the fixed cells were washed twice with PBS, stained with PI solution (50 mg/ml PI, 0.1 mg/ml RNase A and 0.05% triton X-100) for 30 min in the dark. Finally, at least 7000 events per sample were acquired by a flow cytometer (BD, Becton, Dickinson and Co., Piscataway, NJ).

Assessment of changes in MMP by JC-1 staining

Cells were seeded in 6-well plates at a density of 2×10^5 cells per well. After attachment, cells were treated with different concentrations of TPL, and 10 $\mu mol·l^{-1}$ DDP only or combined with 40 $nmol·l^{-1}$ TPL. MMP was detected with JC-1 cationic dye according to the manufacturer's instructions. In brief, treated cells were labelled with JC-1 dye for 30 min. After labelling, cells were washed twice with cold JC-1 dyeing buffer (Widlansky et al., 2010); cells were observed under a U-HGLGPS fluorescent microscope (Olympus). The software for image analysis pro-plus 6.0 was used to analyse the fluorescence intensity of JC-1 staining, and the ratio of red to green was calculated. The experiment was repeated three times.

Western blot analysis

The cells were plated in 6-well culture dishes at a density of 6×10^5 cells/well. The harvested cells were then lysed on ice for 30 min in 100 ml of lysis buffer (120 $mmol·l^{-1}$ NaCl, 40 $mmol·l^{-1}$ Tris (pH 8), 0.1% NP40) and centrifuged at 8600 g for 30 min. The protein concentrations were then measured by bicinchoninic acid (BCA) protein assay. Equal amounts of proteins were electrophoresed through denaturing polyacrylamide gels, transferred onto polyvinylidene difluoride membranes and probed with primary antibodies against Mcl-1, Bcl-2, Bax and caspase-9 at 4 °C overnight. After being washed with TPBS, the membranes were incubated with peroxidase-conjugated secondary antibodies for 2 h. The blots were detected with immobilon western chemiluminescent HRP substrate (Millipore, Darmstadt, Germany) following the manufacturer's instructions. β-actin was used as a loading control.

Statistical analysis

The results were analysed statistically using the SPSS software (Version 17.0) and data were expressed as means ± standard deviations (SD). One-way analysis of variance (ANOVA) with LSD test was employed to identify significant differences ($P < 0.05$ and $P < 0.01$) between the data sets.

Results

Proliferation inhibition induced by TPL in HNE1/DDP cells

The present study evaluated growth of the HNE1/DDP NPC cell line after the treatment with TPL at various concentrations (0–80 $nmol·l^{-1}$) and time points (24–48 h). The results from MTT assays revealed that the cell viability was decreased in a dose- and time-dependent manner following exposure to TPL (Fig. 2A). The MTT assays indicated that the HNE1/DDP cell line was resistant to DDP, since its IC_{50} was 22.9 $\mu mol·l^{-1}$ for 48 h (Fig. 2B). The HNE1/DDP cells treated with TPL exhibited cell swelling, shrinkage, nuclear condensation and fragmentation, and the changes became more serious with the increasing concentration (from 20 $nmol·l^{-1}$ to 80 $nmol·l^{-1}$), as shown in Fig 2C. These results demonstrated that TPL could inhibit proliferation of the HNE1/DDP cells.

Apoptosis induced by TPL in the HNE1/DDP cell line

To further investigate the cytotoxicity of TPL against the HNE1/DDP cells, the cells were subjected to in-
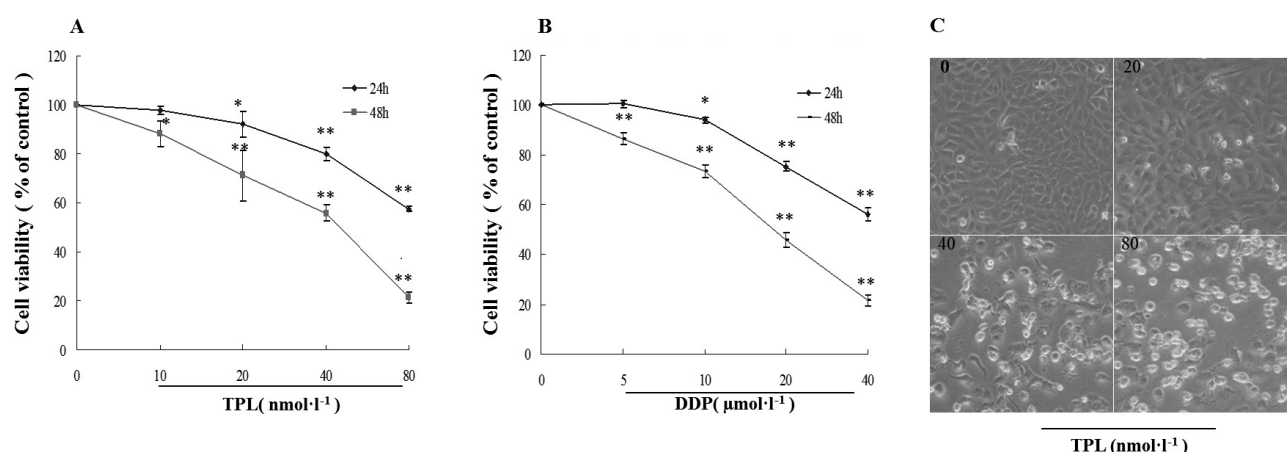
Fig. 2. Proliferation inhibition induced by TPL in the HNE1/DDP cell line
(**A**) HNE1/DDP cells were exposed to varying concentrations of TPL (0–80 $nmol·l^{-1}$) for 24–48 h. Cell viability was assessed by MTT assay. (**B**) HNE1/DDP cells were exposed to different concentrations of DDP (5–40 $\mu mol·l^{-1}$) for 24, 48 h. Cell viability was assessed by MTT assay. (**C**) Effect of TPL on cell morphology. HNE1/DDP cells were treated with different concentrations (20–80 $nmol·l^{-1}$) of TPL for 24 h and the cellular morphology was observed with a camera (×200). *$P < 0.05$ and **$P < 0.01$ *vs* control

creased concentrations of TPL for 24 h, followed by cell apoptosis assessment by flow cytometry with PI staining. TPL treatment induced apoptosis in most DDP-resistant cells, and the proportion of apoptosis increased with elevated TPL concentrations (Fig. 3). The results showed that TPL could induce cell apoptosis in HNE1/DDP cells.

Apoptosis induced by TPL dependent on ROS generation

To explore the possible mechanism of TPL-induced apoptosis in HNE1/DDP cells we measured the generation of ROS. As shown in Fig. 4A, TPL exposure resulted in a time- and concentration-dependent ROS accumulation in the HNE1/DDP NPC cells compared to the control cells. Significant ROS generation was observed when the cells were treated for as little as 1 h, indicating rapid generation of ROS in the TPL-treated cells. However, the production of ROS caused by TPL was abolished by pre-treatment with NAC due to its ability to elevate intracellular glutathione to prevent production of ROS (Fig. 4A). Furthermore, the PI staining analyses revealed that the reduction of ROS by NAC attenuated the number of TPL-induced apoptotic cells from 31.6 % to 8.5 % (Fig. 4B). Collectively, these data suggested that apoptosis induced by TPL is associated with ROS generation.

MMP and the expression of Bcl-2, Mcl-1, Bax, caspase-9 regulated by TPL

During the staining experiments, JC-1 accumulates within the intact mitochondria to form multimer J-aggregates, which results in a change of fluorescence from green to red. Conversely, when apoptosis occurs in the cells, MMP decreases and the multimer J-aggregates are reduced, shifting the fluorescence from red to green. The intensity ratio of red to green was therefore used to evaluate the MMP and early stages of cell apoptosis. As shown in Fig. 5A and 5B, in HNE1/DDP cells treated with TPL at concentrations 0–80 nmol·l^{-1} for 24 h, the red fluorescence weakened while the green fluorescence got stronger, and the ratio of red to green decreased. The results showed that TPL could induce depolarization of the mitochondrial membrane and lower the MMP. When the cells underwent apoptosis, relative protein changes were always involved. Western blot showed that TPL reduced expression of anti-apoptotic Bcl-2 and Mcl-l but increased the pro-apoptotic Bax and caspase-9 (Fig. 5C). As it is known that MMP, Bcl-2, Mcl-1, Bax and caspase-9 all are part of mitochondrial pathways of cell apoptosis, the results indicated that TPL could induce HNE1/DDP cell apoptosis by regulating the mitochondrial pathways.

Improved cytotoxicity of the synergistic combination of TPL and DDP in DDP-resistant HNE1/DDP cells

The present study tested whether low doses of TPL and DDP in combination were able to exert a synergistic anticancer effect, and also investigated its possible mechanism. Using 10 μmol·l^{-1} DDP in combination with 40 nmol·l^{-1} TPL, the inhibition rate rapidly increased to 81.30 % after 48 h (Fig. 6A). DDP alone (10 μmol·l^{-1}) induced 26.5 % cell death (Fig. 6A). The combination index (CI) of the combination was < 1, suggesting that
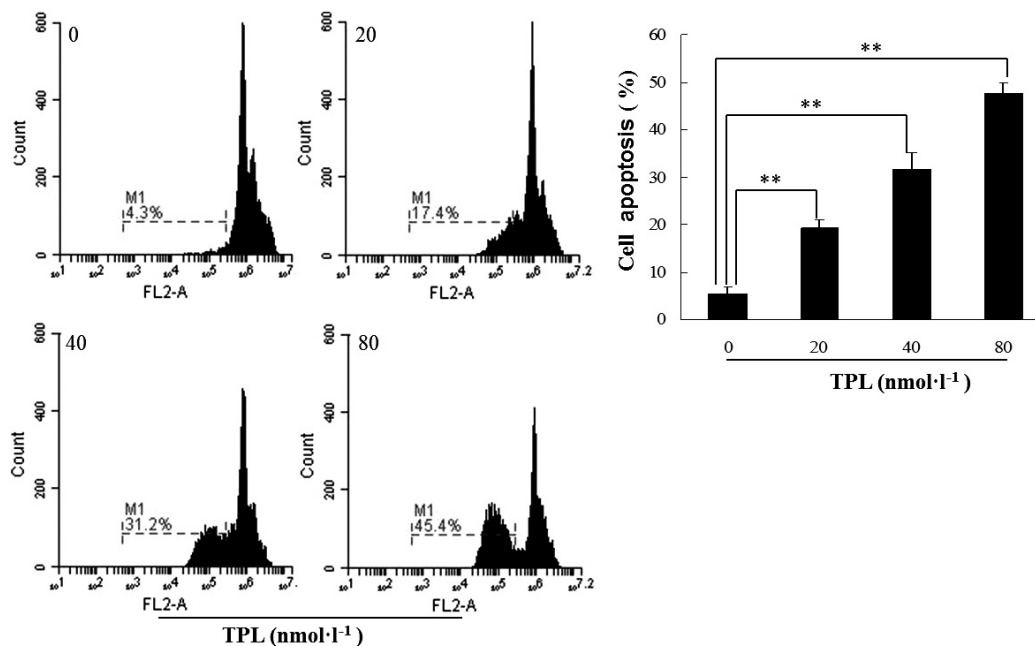
Fig. 3. Cell apoptosis induced by TPL in HNE1/DDP cells
HNE1/DDP cells were cultured for 24 h with varying doses of TPL (20–80 nmol·l^{-1}). Apoptosis was identified by PI staining and analysed by flow cytometry. **P < 0.01 *vs* control
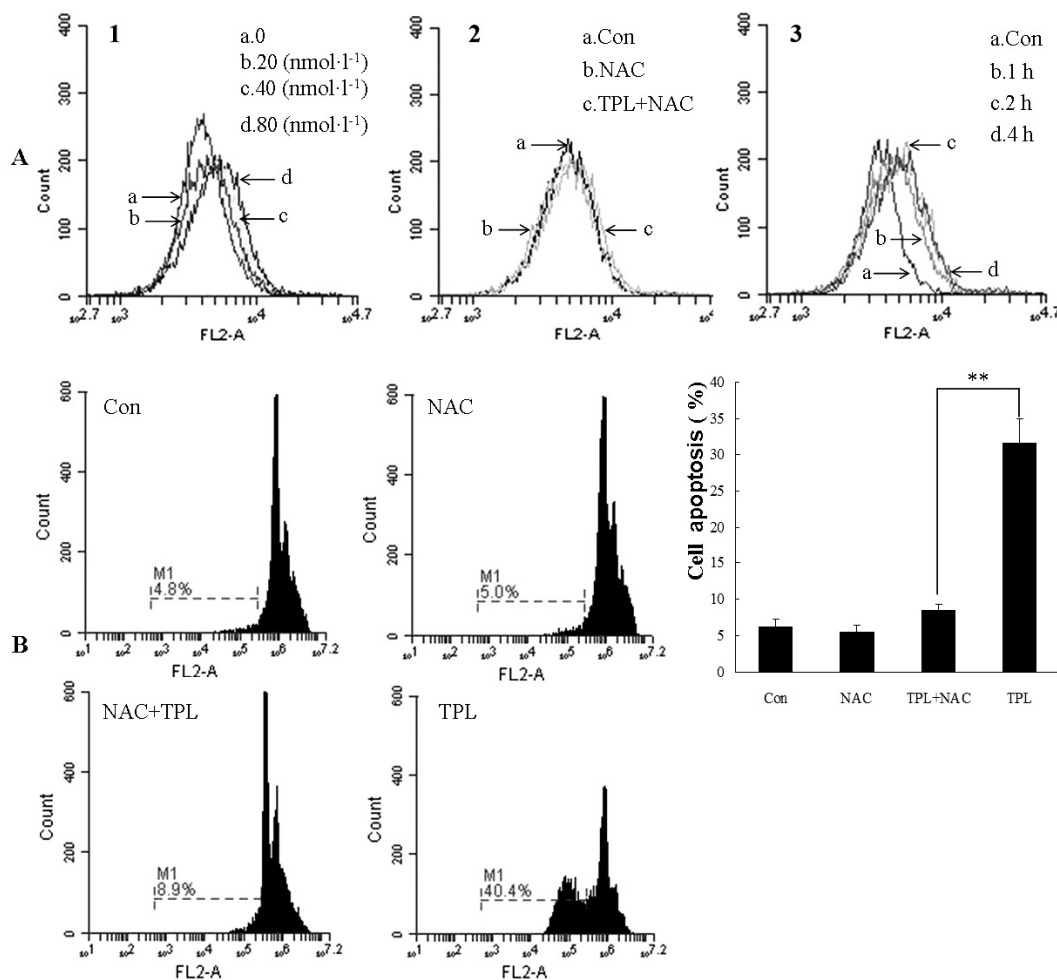
Fig. 4. TPL induced cell apoptosis via ROS generation in HNE1/DDP cells.
(**A**) TPL induced ROS accumulation in HNE1/DDP cells. (**1**) Cells were incubated with TPL in concentrations 20–80 nmol·l^{-1} for 2 h and stained with ROS fluorescent probe DHE. ROS production was measured by flow cytometry. (**2**) Cells were pre-incubated with 5 mmol·l^{-1} NAC for 1 h, incubated with 80 nmol·l^{-1} TPL for 2 h and then analysed for the ROS content. (**3**) Cells were incubated with 80 nmol·l^{-1} TPL for 1, 2 and 4 h and ROS production was measured. (**B**) TPL-induced apoptosis was abolished by NAC. Cells were pre-incubated with 5 mmol·l^{-1} NAC for 1 h and/or incubated with 40 nmol·l^{-1} TPL for 24 h. Apoptosis was identified by PI staining and analysed by flow cytometry. **P < 0.01 *vs* TPL

the antiproliferative effect of the combination was synergistic. Additionally, the colony-forming assay confirmed that TPL enhanced the antiproliferative effect of DDP (Fig. 6B). The MMP and Bcl-2, Mcl-1, Bax and caspase-9 were also assessed in the combination group. As shown in Fig. 6C and 6D, the MMP and Bcl-2, Mcl-1 were reduced, but Bax and caspase-9 levels were increased in the combination group compared to control. These observations demonstrated that TPL combined with DDP exhibited a synergistic effect against DDP-resistant NPC cells and that this effect may be related to mitochondrial pathways mediated by TPL.

Discussion

Even though DDP chemotherapy and radiotherapy are the main treatments for NPC, many NPC patients do not benefit much from concurrent chemoradiotherapy (Ye et al., 2014). Drug resistance has emerged as the major impediment to effective NPC therapy. Thus, novel strategies that either have an effective anti-tumour effect on NPC employing new mechanisms or are able to enhance the effects of DDP are highly desirable. In the present study, TPL, a monomer of Chinese traditional herbs, was used in DDP-resistant NPC cells to detect its anti-tumour effect alone or in combination with DDP.

The pleiotropic anticancer activities of TPL have attracted a great deal of research interest. Notably, TPL has also been identified to be effective in the induction of apoptosis in many cancer cells, including some drug-resistant cancer cells, such as bladder cancer (Ho et al., 2015), ovarian cancer (Zhong et al., 2013), myeloid leukaemia (Chen et al., 2013), and pancreatic cancer (Zhu et al., 2012). The results of the present study demonstrated that TPL also displays activity against DDP-resistant NPC and synergizes with DDP in DDP-resistant NPC cells.

ROS are involved in the regulation of cell apoptosis through various stimuli. When cells are exposed to apoptotic stimuli, ROS are generated and induce opening

A

B

C
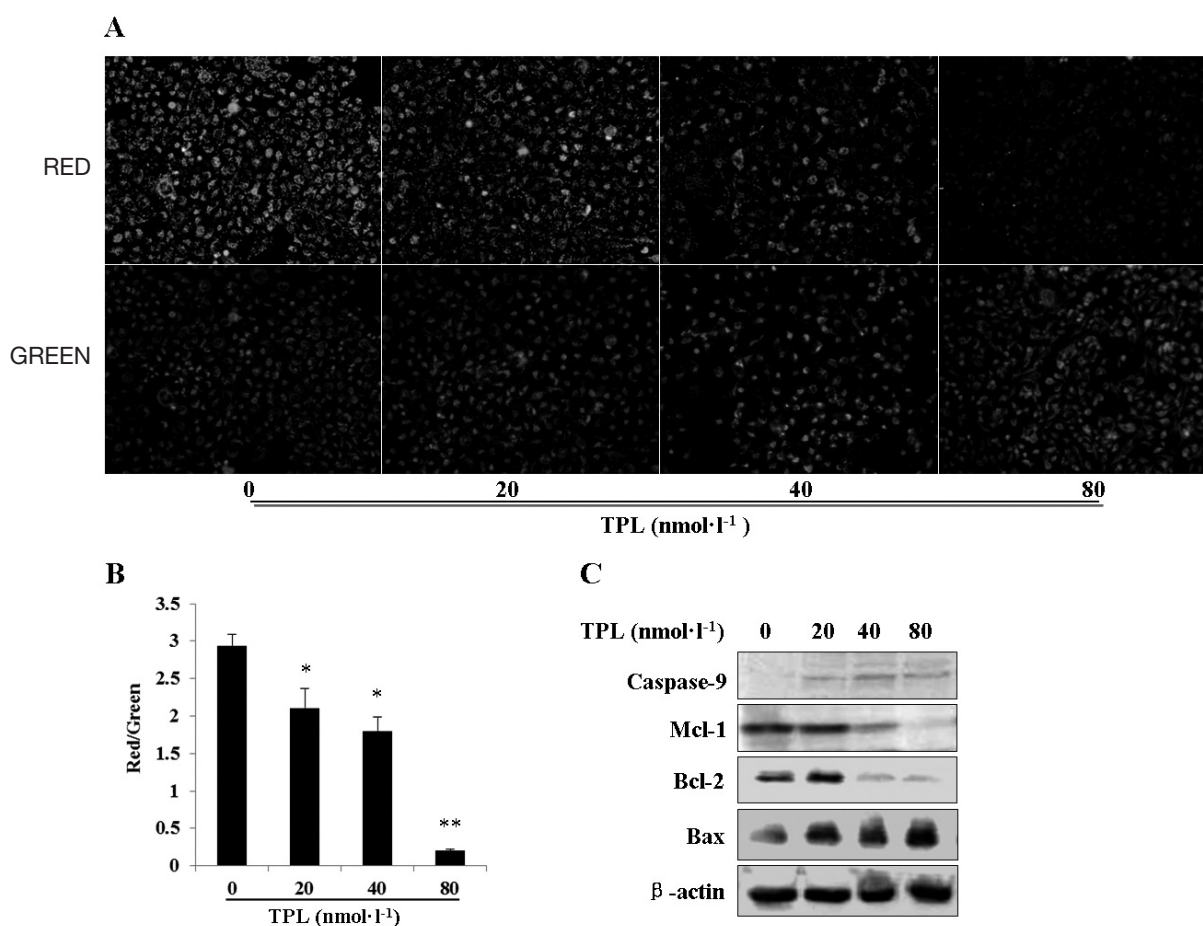
Fig. 5. TPL triggered the mitochondrial pathway.
(**A**) TPL reduced MMP in HNE1/DDP cells. HNE1/DDP cells were incubated with TPL in the concentrations 20–80 nmol·l⁻¹ for 24 h, stained with JC-1 for 30 min, and then observed under a fluorescence microscope. (**B**) The fluorescence intensity ratio of red to green of A. *P < 0.05, **P < 0.01 *vs* 0 nmol·l⁻¹ group, the data represented three independent experiments. (**C**)The effects of TPL on the expression of Bcl-2, Mcl-1, Bax and caspase-9 were evaluated by Western blot. HNE1/DDP cells were cultured with TPL in concentrations 20–80 nmol·l⁻¹ for 24 h, then analysed by Western blot.

of the mitochondrial permeability transition pores, release of pro-apoptotic proteins, and activation of caspase-9 (Rasola and Bernardi, 2014). The present study suggested that ROS accumulation contributed to TPL-induced cell apoptosis in HNE1/DDP NPC cells. Previously, it has been reported that elevated intracellular ROS mediates TPL-induced apoptosis in human breast cancer and DDP-resistant human ovarian cancer cells (Zhong et al., 2013), which is in agreement with the findings of the present study. Although a possible contribution of ROS has been observed in the apoptotic response to TPL, the role of ROS generation in cell apoptosis induced by TPL is unclear. Mitochondria are a major source of cellular ROS. Evidences showed that reducing the ROS level could block the loss of MMP in a model of activated cell apoptosis (Bonora et al., 2014). Bcl-2, Mcl-1 and Bax belong to the Bcl-2 family and play an anti- and pro-apoptotic role in the intrinsic apoptosis pathway, respectively. Bax is a pro-apoptotic protein, which triggers cytochrome c leaking from mitochondria and activation of caspase-9. Bcl-2 can block the action of Bax by activation of its homo-oligomeriza-

tion. Mcl-1 displays the same anti-apoptotic effect as Bcl-2. Caspase-9 is the main protein of the mitochondrial pathways and when activated, the cells die by apoptosis through mitochondrial pathways. MMP and the related proteins (Bcl-2, Mcl-1, Bax and caspase-9) were also examined in the present study. The results suggested that increased expression of Bax and caspase-9 and declined levels of Bcl-2 and Mcl-1 may contribute to the apoptosis-promoting activity of TPL in the HNE1/DDP NPC cells. All the above-mentioned data indicated that apoptosis induced by TPL in HNE1/DDP cells was dependent on the mitochondrial pathways regulated by ROS accumulation.

Numerous commonly used chemotherapy agents, including DDP, could trigger the ROS-dependent activation of apoptosis (Penney et al., 2013). However, continuous DDP treatment may reduce the cellular ROS levels, and cancer cells containing reduced ROS may become drug resistant (Indran et al., 2011; Sosa et al., 2013). Furthermore, an elevation of the cellular ROS level by exogenous ROS generation in combination with DDP re-sensitizes drug-resistant cancer cells.
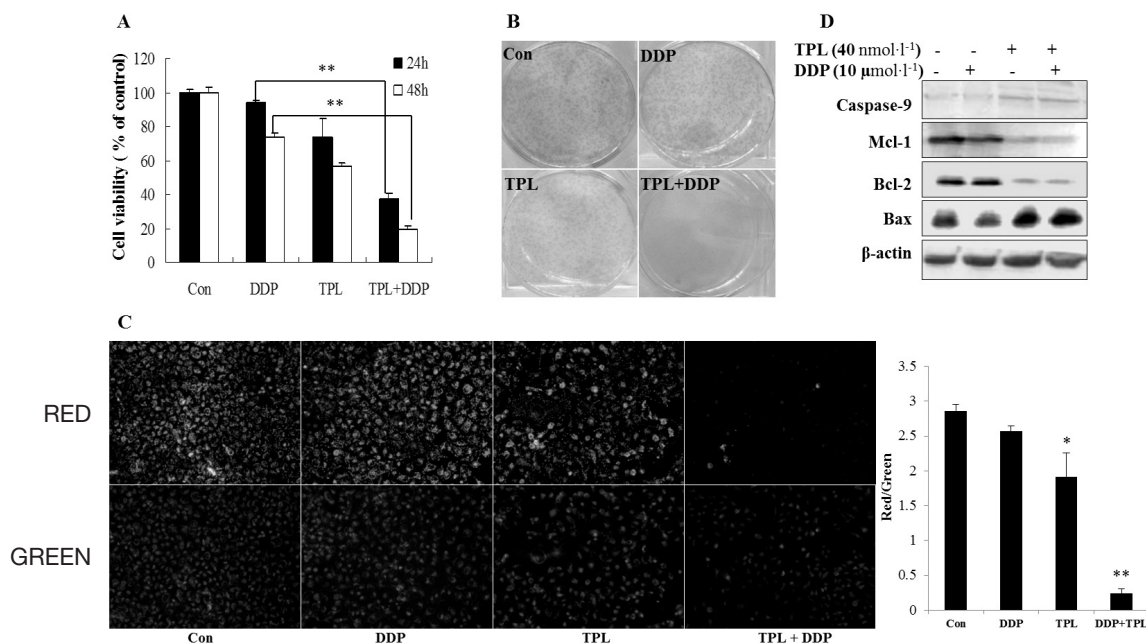
Fig. 6. TPL sensitized HNE1/DDP cells to DDP *in vitro*.
(**A**) Cell viability. Cells were treated with 10 μmol·l⁻¹ DDP or 40 nmol·l⁻¹ TPL alone or in combination for 24 h, 48 h. Cell viability was assessed by MTT assay, the data were presented as the mean ± SD of three independent experiments (**P < 0.01 *vs*. the combination group). (**B**) Colony-forming assay. (**C**) MMP determined by JC-1 staining after the cells were treated for 24 h. *P < 0.05, **P < 0.01 *vs* control, the data represented three independent experiments. (**D**) Western blot analysis of caspase-9, Mcl-1, Bcl-2 and Bax in HNE1/DDP cells treated with 10 μmol·l⁻¹ DDP and/or 40 nmol·l⁻¹ TPL for 24 h.

Previous reports (Tan et al., 2013) and the present studies indicated that TPL can induce ROS generation. Hence, TPL combined with DDP can restore the sensitivity of HNE1/DDP cells to DDP. The possible mechanism may be that ROS generation induced by TPL activated the mitochondrial pathways and induced apoptosis.

Altogether, these findings indicate that TPL has triggered ROS generation, which is a critical mediator of TPL-induced cell apoptosis in DDP-resistant NPC cells. We showed that TPL induced cell apoptosis and exhibited **a** synergistic effect with DDP in DDP-resistant HNE1/DDP NPC cells. Further *in vivo* experiments may aid in the confirmation of the therapeutic efficacy of this agent for patients with DDP-resistant NPC.

References

Alsaied, O. A., Sangwan, V., Banerjee, S., Krosch, T. C., Chugh, R., Saluja, A., Vickers, S. M., Jensen, E. H. (2014) Sorafenib and triptolide as combination therapy for hepatocellular carcinoma. *Surgery* **156**, 270-279.

Bao, L. L., Hazari, S., Mehra, S., M., Kaushal, D., Moroz, K., Dash, S. (2012) Increased expression of P-glycoprotein and doxorubicin chemoresistance of metastatic breast cancer is regulated by miR-298. *Am. J. Pathol.* **180**, 2491-2503.

Bonora, M., Pinton, P. (2014). The mitochondrial permeability transition pore and cancer: molecular mechanisms involved in cell death. *Front. Oncol.* **4**, 302.

Chen, F., Liu, Y., Wang, S*.,* Guo, X., Shi, P., Wang, W., Xu, B. (2013) Triptolide, a Chinese herbal extract, enhances drug sensitivity of resistant myeloid leukemia cell lines through downregulation of HIF-1α and Nrf2. *Pharmacogenomics* **14**, 1305-1317.

Deeb, D., Gao, X., Jiang, H., Janic, B., Arbab, A. S., Rojana-sakul, Y., Dulchavsky, S. A, Gautam, S. C. (2010) Oleanane triterpenoid CDDO-Me inhibits growth and induces apoptosis in prostate cancer cells through a ROS-dependent mechanism. *Biochem. Pharmacol.* **79**, 350-360.

Feng, X., Zhang, Q., Xia, S., Zhang, Y., Deng, X., Su. W., Huang, J. (2014) MTA1 overexpression induces cisplatin resistance in nasopharyngeal carcinoma by promoting cancer stem cells properties. *Mol. Cells* **37**, 699-704.

Ho, J. N., Byun, S.S., Lee, S., Oh, J. J., Hong, S. K., Lee, S. E., Yeon, J. S. (2015) Synergistic antitumor effect of triptolide and cisplatin in cisplatin resistant human bladder cancer cells. *J. Urol.* **193**, 1016-1022.

Indran, I. R., Tufo, G., Pervaiz, S., Brenner, C. (2011) Recent advances in apoptosis, mitochondria and drug resistance in cancer cells. *Biochim. Biophys. Acta* **1807**, 735-745.

Li, C., Chu, C.-Y., Huang L.-H., Wang, M. H., Sheu, L. F., Yeh, J. I., Hsu, H. Y. (2012) Synergistic anticancer activity of triptolide combined with cisplatin enhances apoptosis in gastric cancer in vitro and in vivo. *Cancer Lett.* **319**, 203-213.

Li, X. J. Y., Jiang, Z. Z., Zhang, L. Y. (2014) Triptolide: Progress on research in pharmacodynamics and toxicology. *J. Ethnopharmacol.* **155**, 67-79.

Liu, Q. Y. (2011) Triptolide and its expanding multiple pharmacological functions. *Int. Immunopharmacol.* **11**, 377-383.

Marquitz, A. R., Raab-Traub, N. (2012) The role of miRNAs and EBV BARTs in NPC. *Semin. Cancer Biol.* **22**, 166-172.

Pan, Y., Zhang, Q., Atsaves, V., Yang, H., Claret, F. X. (2013) Suppression of Jab1/CSN5 induces radio- and chemo-sensitivity in nasopharyngeal carcinoma through changes to the DNA damage and repair pathways. *Oncogene* **32**, 2756-2766.

Penney, R. B., Roy, D. (2013) Thioredoxin-mediated redox regulation of resistance to endocrine therapy in breast cancer. *Biochim. Biophys. Acta* **1836**, 60-79.

Rasola, A., Bernardi, P. (2014). The mitochondrial permeability transition pore and its adaptive responses in tumor cells. *Cell Calcium* **56**, 437-445.

Sosa, V., Moline, T., Somoza, R., Paciucci, R., Kondoh, H., Leonart, M. E. (2013) Oxidative stress and cancer: an overview. *Ageing Res. Rev.* **12**, 76-90.

Su, W. P., Hsu, S. H., Wu, C. K., Chang, S. B., Lin, Y. J., Yang, W. B., Hung, J. J., Chiu, W. T., Tzeng, S. F., Tseng, Y. L., Chang, J. Y., Su, W. C., Liaw, H. (2014) Chronic treatment with cisplatin induces replication-dependent sister chromatid recombination to confer cisplatin-resistant phenotype in nasopharyngeal carcinoma. *Oncotarget* **5**, 6323-6237.

Sun, X. J., Zhang, P., Li, H. H., Jiang, Z. W., Jiang, C. C., Liu, H. (2014) Cisplatin combined with metformin inhibits migration and invasion of human nasopharyngeal carcinoma cells by regulating E-cadherin and MMP-9. *Asian Pac. J. Cancer Prev.* **15**, 4019-4023.

Tan, B. J., Chiu, G. N. (2013) Role of oxidative stress, endoplasmic reticulum stress and ERK activation in triptolide-induced apoptosis. *Int. J. Oncol.* **42**, 1605-4612.

Widlansky, M. E., Wang, J. L., Shenouda, S. M., Hagen, T. M., Smith, A. R., Kizhakekuttu, T. J., Kluge, M. A.,

Weihrauch, D., Gutterman, D. D., Vita, J. A. (2010) Altered mitochondrial membrane potential, mass, and morphology in the mononuclear cells of humans with type 2 diabetes. *Transl. Res.* **156**, 15-25.

Ye, C. S., Zhou, D. N., Yang, Q. Q., Deng, Y. (2014). Silencing SATB1 influences cell invasion, migration, proliferation, and drug resistance in nasopharyngeal carcinoma. *Int. J. Clin. Exp. Pathol.* **7**, 914-922.

Zhong, Y. Y., Chen, H. P., Tan, B. Z., Yu, H. H., Huang, X. S. (2013) Triptolide avoids cisplatin resistance and induces apoptosis via the reactive oxygen species/nuclear factor-κB pathway in SKOV3 platinum-resistant human ovarian cancer cells. *Oncol. Lett.* **6**, 1084-1092.

Zhou, Y. F., Sridhar, R., Shan, L., Sha, W., Gu, X., Sukumar, S. (2011) Loperamide, an FDA-approved antidiarrhea drug, effectively reverses the resistance of multidrug resistant MCF-7/MDR1 human breast cancer cells to doxorubicin-induced cytotoxicity. *Cancer Invest.* **30**, 119-125.

Zhu, W., Li, J., Wu, S., Li, S., Le, L., Su, X., Qiu, P., Hu, H., Yan, G. (2012) Triptolide cooperates with cisplatin to induce apoptosis in gemcitabine-resistant pancreatic cancer. *Pancreas* **41**, 1029-1038.